# Impulsive Solar X-Ray Bursts: Bremsstrahlung Radiation from a Beam of Electrons in the Solar Chromosphere and the Total Energy of Solar Flares

by

Vahé Petrosian

June 1973



SUIPR Report No. 528

National Aeronautics and
Space Administration
Grant NGL 05-020-272


INSTITUTE FOR PLASMA RESEARCH
STANFORD UNIVERSITY, STANFORD, CALIFORNIA

# IMPULSIVE SOLAR X-RAY BURSTS: BREMSSTRAHLUNG RADIATION FROM A BEAM OF ELECTRONS IN THE SOLAR CHROMOSPHERE AND THE TOTAL ENERGY OF SOLAR FLARES

by

Vahé Petrosian*

National Aeronautics and Space Administration
Grant NGL 05-020-272

SUIPR Report No. 528

June 1973

Institute for Plasma Research
Stanford University
Stanford, California

---

*Alfred P. Sloan Foundation Fellow

Page Intentionally Left Blank

## ABSTRACT

Analysis of various aspects of impulsive x-ray bursts (IXB's) has lead us to consider a model where the x-rays are produced by Bremsstrahlung radiation from a beam of electrons directed toward the photosphere. We find that in general the x-ray spectrum from such a beam will fall off more rapidly than when the effect of the beaming of radiation is neglected. Furthermore, the spectral index of the resulting x-rays appears to increase by about unity for x-ray energies $> 100$ kev, a fact which may explain the observed cutoff in the spectrum of the IXB's. It is also shown that in such a model there is sufficient energy in the form of non-thermal electrons to explain the total energy ($\sim 10^{32}$ ergs) of a flare.

# I. INTRODUCTION

Observation of impulsive hard x-ray and microwave bursts provide direct evidence that high energy particles play a major role in the energetics of solar flares. The purpose of this communication is to examine the feasibility of the postulate that most of the observed electromagnetic radiation from flares is a result of the interaction with the solar chromospheric and coronal plasma of a beam of high energy (non-thermal) electrons which are accelerated somewhere in the corona (see, for example Sturrock 1968; de Jager and Kundu 1963). In such a model the impulsive x-ray bursts (IXB's) are produced by bremsstrahlung and the microwave bursts by gyro-synchrotron radiation. However, most of the energy of the non-thermal electrons goes into heating (or evaporation) of the ambient plasma through elastic scattering with thermal electrons and through ionization. All other observed electromagnetic radiation (such as soft x-rays, XUV, optical) of a flare is a result of cooling of the plasma. Some aspects of such a model have been discussed by Syrovatskii and Shmeleva (1973).

In Section II we discuss the decay rate of non-thermal electrons in the solar chromosphere and compare it with the observed decay rates of IXB's. We find that injection of non-thermal electrons is not instantaneous but rather occurs continuously throughout the impulsive phase. In Section III we calculate the expected x-ray spectrum from the interaction of a beam of high energy particles with the plasma in a stratified atmosphere. In Section IV we discuss the total energy of a flare in the form of non-thermal electrons. We find that this energy is sufficient to account for all the observed radiation from a flare. A brief discussion of the results of the paper is presented in Section V.

## II. DECAY RATES

Until recently most analyses of the impulsive phase of solar flares have dealt with interaction of an isotropic distribution of non-thermal electrons with a homogeneous medium (cf. e.g. Takakura and Kai, 1966; Takakura, 1969; Kane and Anderson, 1970). In such models, the extent of the homogeneous region must be at least as large as the electron mean free path, $\lambda \sim 10^{22}/n_o$, where $n_o$ is the density of electrons in the ambient plasma (cf. equation (4) below). For a density of $n_o \leqslant 10^{12}\text{cm}^{-3}$, $\lambda$ is greater than $10^5$km which is much larger than the density scale height at heights of $h < 10^5$km above the photosphere. Thus, unless the particles are trapped in a much smaller region the homogeneous model is not tenable.

If the non-thermal particles are injected impulsively into and are trapped in a small homogeneous cloud of hydrogen plasma with density $n$ their energy loss rate due to elastic collision is given by

$$-\dot{E}_{coll} = 2\pi r_o^2 n\, c\, \ell n\Lambda/\beta \,, \tag{1}$$

where for ionized hydrogen (Ginzburg and Syrovatskii, 1964; Hayakawa and Kiato, 1956)

$$\Lambda_i \approx \beta^4\gamma/[\pi\, \alpha\, n(\hbar/mc)^3] \tag{2}$$

and for atomic hydrogen

$$\Lambda_a \approx 2(\gamma-1)\beta^2\gamma^2/\alpha^4 \,. \tag{3}$$

Here $\alpha = \frac{1}{137}$, $r_o = e^2/mc^2 = 2.8 \times 10^{-13}$cm, $\beta$ is the velocity in units of speed of light, $\gamma$ is the Lorentz factor or the total electron energy in units of electron rest-mass energy $mc^2$, and $E = (\gamma - 1)$ is the kinetic energy of the electrons in units of $mc^2$ (all energies will be in units of

$mc^2$ unless otherwise specified). The "lifetime" $\tau$ and the "mean free path" $\lambda$ of the electrons are given by

$$\lambda(E) = c\beta\,\tau(E) \equiv -c\beta E/\dot{E}_{coll} = \frac{E\beta^2}{2\pi r_o^2 n\,\ell n\Lambda} \quad . \tag{4}$$

The lifetime of the non-relativistic electrons ($E \ll 1$) which are responsible for 10 to 100 kev IXB's, $\tau(E) \propto E\beta \approx 2\,E^{3/2}$. This implies hardening of the spectrum of an IXB with time which is contrary to observations (Kane and Anderson, 1970). Furthermore, in such models the observed cutoff (for photon energies > 70 kev) in the spectrum of IXB's (Frost, 1969; Kane and Anderson, 1970) implies absence of electrons with energies > 100 kev. However, electrons of such energies are necessary for production of the microwave bursts which are observed simultaneously with IXB's (Holt and Ramaty, 1969; Takakura, 1972).

We see that if the non-thermal electrons are not trapped as mentioned above, the assumption of a homogeneous medium is incorrect. Some of the electrons are directed toward the photosphere and perhaps some away from the sun. The latter particles escape almost freely into the interplanetary medium (except perhaps for some type III radio emission; Kane, 1972). The electrons beamed toward the photosphere penetrate into higher density regions, interact strongly with the solar plasma, and produce (directly or indirectly) the bulk of the observed radiation from flares. Exactly what fraction of particles escape and what fraction lose their energy in the solar plasma depends on the details of the structure of magnetic field and condition of plasma in the region of acceleration, which are not well known. However, for understanding of IXB's only the interaction of particles beamed toward the photosphere is important. We therefore consider the interaction with the solar plasma of a beam of high energy electrons directed toward the sun, and for the purpose of illustration we neglect first the presence of magnetic

field (which will be a good approximation if the particles have small pitch angles, as expected from acceleration of particles in a current sheet; cf. Speicer, 1965) and characterize the ambient plasma (assumed to be pure hydrogen, a fraction $f$ of which is ionized) density variation with a density scale height $H$. Both $H$ and $f$ vary much more slowly than the total density:

$$n_p = f\,n\ , \quad n_H = (1-f)n\ ,$$
$$n = n_o e^{s/H}\ , \tag{5}$$

where $n_o$ is the density at the point of injection and $s$ is distance along the electron path away from this point. The range $s(E) = \int_E^o (dE/ds)^{-1} dE$ of an electron with initial energy $E$ is obtained from integration of equations (1) and (2):

$$\frac{E^2}{1+E} = 2\pi r_o^2 \int_o^{s(E)} \ell n\Lambda\ n\,ds\ , \tag{6}$$

where $\Lambda = \Lambda_i^f + \Lambda_a^{1-f}$ (cf. eqs. 1 and 5). For a constant scale height and $\Lambda$, equation (6) gives

$$s(E) = H\,\ell n\left[1 + \frac{\lambda_o(E)}{H}\left(\frac{2+E}{1+E}\right)\right] \tag{7}$$

where $\lambda_o(E)$ is the mean free path at the acceleration region, $s = 0$ ($n = n_o$ in equation 2). According to these relations, electrons of different energy lose their energy at different places in the solar chromosphere. $s(E)$ gives the approximate distance of the energy loss region from the acceleration region. Most of the energy is lost within the last few scale heights, so that electrons of energy $E$ deposits most of its energy at a region with a density $n$ such that[1]

[1] This condition justifies the assumption of constancy of $\Lambda$ made in deriving equation (7). For ionized plasma, for all ranges of energy $E$, $\Lambda_i$ can be approximated (cf. Ginzburg and Syrovatskii, 1964) as

$$\Lambda_i \propto \frac{E^2}{n(1+E)} \times \left(\frac{E+2}{E+0.4}\right) \propto H\ .$$

$$\frac{E^2}{n(1+E)} \approx \text{const.} = 2\pi r_o^2 H \ell n\Lambda \ . \qquad (8)$$

For low energy electrons the mean free path $\lambda_o(E) \ll H$ so that $s(E) = \lambda_o(E)$ as expected, since the medium looks homogeneous to low energy particles. The lifetime of these particles is therefore given by equation (4). The higher energy particles penetrate deeper into higher density regions where they lose energy faster than would be expected from equation (4).

In general an exact relation between particle lifetime and energy can be obtained in a similar manner. This relationship is complicated, but for most practical purposes we can approximate it as

$$\tau(E) \approx \frac{s(E)}{c\beta} \approx \frac{H}{v} \ell n\left[1 + \frac{\lambda_o(E)}{H}\left(\frac{2+E}{1+E}\right)\right], \qquad (9)$$

because through most of their paths the particles travel with their initial energy or velocity $v$. For the conditions in the solar chromosphere $Hn_o \sim 10^{18}$ to $10^{19}\text{cm}^{-2}$ the maximum lifetime is $\tau_{max} \approx 4H/v$ and occurs for $\lambda_o(E) \approx 25\ H$ or for particle energy (non-relativistic)

$$E_c \approx \left[25\ \pi r_o^2 \ell n\Lambda\ n_o H\right]^{1/2} \approx 8.4\ \text{kev}\left(n_o H/10^{18}\text{cm}^{-2}\right)^{1/2} \ . \qquad (10)$$

Thus, the maximum lifetime is

$$\tau_{max} \approx 0.07\ \text{sec}\left(\frac{H}{10^8\text{cm}}\right)\left(\frac{n_o H}{10^{18}\text{cm}^{-2}}\right)^{-1/4} \ . \qquad (11)$$

Since the scale height in the lower corona and chromosphere can rarely exceed $10^4$ km, the lifetime of electrons is much shorter than the observed decay rate of IXB's ($\sim$ 2-10 sec) which implies that the particle acceleration continues throughout the duration of IXB's. Variation of $\tau$ with energy is plotted on Figure 1 for various values of scale height and density $n_o$.

It is evident that the decay time would approach the observed value (a few seconds) only for very large values of the scale height.

Note that if the particle path makes an angle $\theta$ with respect to the radial direction, the scale height in all our equations must be multiplied by $\sec\theta \leqslant 1 + (h/R_\odot)^2$ where $h$ is the height above the photosphere of the acceleration region and $R_\odot$ is the radius of the sun. Similarly if the particles travel along magnetic lines of force with a pitch angle $\Psi$, the scale height must be multiplied by $\frac{1}{\cos\Psi}$ which is of order unity unless $\Psi \approx \frac{\pi}{2}$. Particles with such large pitch angles will be trapped between mirror points in the low density acceleration region until they collide with an ambient electron as a result of which their pitch angle changes and they penetrate into the chromosphere along the magnetic field lines. As shown by Benz and Gold (1971), the time scale for change in pitch angle (like the collision or deflection time scale) is proportional to $E^{3/2}$ (Spitzer, 1956) so that models where the initial pitch angles are not small, encounter the same difficulty with the decay time of IXB's as the trapped model discussed above. The small pitch angle particles under consideration here will not be trapped, because the scale height for the magnetic field is much larger than the density scale height. We therefore can neglect the presence of the magnetic field.

## III. SPECTRUM OF HARD X-RAY BURSTS

In this section we calculate the x-ray spectrum resulting from the interaction of a beam of high energy electrons with the chromospheric plasma. This spectrum will depend on the angle between the beam and the line of sight. We therefore consider the effect of the "relativistic" beaming of the radiation on the observed spectrum.

Since in the model under consideration the electrons responsible for the IXB's are moving primarily toward the sun and away from the observer at the earth, the beaming of the bremsstrahlung radiation will reduce the observed intensity of harder x-rays relative to softer ones. This in turn will affect the derived spectrum of the accelerated electrons, in particular at high energies. Elwert and Huag (1971) have shown that even at non-relativistic energies there is considerable beaming of the radiation in the direction of motion of the particles. They consider this effect for a given electron spectrum in a thin target. As is evident from our discussion above, the electrons responsible for IXB's lose all their energy so that for these electrons radiation in a thick target must be considered. In this case the intensity of bremsstrahlung radiation becomes independent of the value of the ambient plasma density as shown by Brown (1971) and emphasized recently by Hudson (1972).

The rate of energy loss by bremsstrahlung radiation is obtained from the cross section for the emission of photons of energy $k$ (in units of $mc^2$) in the interval $dk$ which can be written as

$$d\sigma = \alpha r_o^2 \left(\frac{d\Omega}{4\pi}\right) \frac{dk}{k} f(E,k,\theta) \ , \qquad (12)$$

where $d\Omega$ is the differential solid angle and $\theta$ is the angle between the

line of sight (direction of emitted photon) and the direction of the motion of the electron. The bremsstrahlung energy loss rate (for photon of energy $k$ in the direction $\theta$) is then given by

$$-\dot{E}_{brem} = d\sigma \; nc\beta \; k \; , \tag{13}$$

so that in the process of slowing down an electron radiates a fraction $Y(E,k,\theta)$ of its energy loss in the form of photons of energy k to k + dk. From equations (1) and (13)[2]

$$Y(E,k,\theta) = \frac{d\Omega}{4\pi}\left(\frac{\alpha}{2\pi \ell n \Lambda}\right)\beta^2 f(E,k,\theta) \; . \tag{14}$$

The energy radiated (in the form of photons of energy $k$ to $k + dk$) by an electron of initial energy $E$ is therefore equal to $(E-k) \times \bar{Y}$, where $\bar{Y}$ is the average value of $Y$ along the path of the electron; or, the bremsstrahlung emissivity (of photons with energies from k to k + dk) per electron of initial energy $E$ is given by

$$\mathcal{E}(E,k,\theta) = \frac{d\Omega}{4\pi}\left(\frac{\alpha}{2\pi \ell n \Lambda}\right)\int_k^E \beta'^2 f(E',k,\theta)dE' \; . \tag{15}$$

Similarly the emissivity integrated over all directions can be written as

$$\mathcal{E}(E,k) = \left(\frac{\alpha}{2\pi \ell n \Lambda}\right)\int_k^E \beta'^2 \; F(E',k)dE' \; , \tag{16}$$

where

$$F(E',k) = \frac{1}{2}\int_o^\pi f(E',k,\theta)\sin\theta \; d\theta \; . \tag{17}$$

[2] We assume here that $|\dot{E}_{brem}| \ll |\dot{E}_{coll}|$ which for an ambient hydrogen gas will be a good approximation if we are limited to electrons with $E < 100$ Mev (see, e.g. Berger and Seltzer, 1964).

The results of integration of equations (15) and (16) are presented on Figures 2a, 2b and 2c, where we plot the ratio

$$R(E,k,\theta) = \frac{\mathcal{E}(E,k,\theta)}{\mathcal{E}(E,k)} \times \left(\frac{4\pi}{d\Omega}\right) \tag{18}$$

versus $\cos\theta$ for various initial electron and photon energies. We have used for the quantities f and F the expressions 2BN and 3BN of Koch and Motz (1959) with the Elwert (1939) coulomb correction.

As is evident from the graphs on Figure 2, the radiation yield at high electron and photon energies depends strongly on the direction $\theta$. These results indicate that the derivation of electron spectrum based on isotropic electron distribution will yield incorrect results if electrons are beamed. The effect of the beaming will of course depend on the direction of the electron beam with respect to the line of sight. (For example, if the electrons are beamed almost radially into the sun, then $\theta \approx \pi$ for flares near the center of the sun and $\theta \approx \pi/2$ for the limb flares.) In order to show the extent of this effect and its dependence on the angle $\theta$, we calculate the expected photon spectrum for various values of $\theta$ and for a power law electron flux

$$dJ_e(E) = K\, E^{-\delta-1}\, dE \ \text{sec}^{-1} \ . \tag{19}$$

The integral and differential spectra of the photon energy fluxes (in units of $mc^2$) are then given by[3]

$$J(k) = \frac{K}{\delta}\left(\frac{\alpha}{2\pi \ell n\Lambda}\right)\int_k^\infty E'^{-\delta}\beta'^2\, F(E',k)dE' \ \text{sec}^{-1} \ ,$$

$$J(k,\theta) = \frac{K}{\delta}\frac{d\Omega}{4\pi}\left(\frac{\alpha}{2\pi \ell n\Lambda}\right)\int_k^\infty E'^{-\delta}\beta'^2\, f(E',k,\theta)dE' \ \text{sec}^{-1} \ . \tag{20}$$

[3]Note that $J(k) = \int_k^\infty \mathcal{E}(E,k)\ dJ_e(E) = K\left(\frac{\alpha}{2\pi \ell n\Lambda}\right)\int_k^\infty dE E^{-\delta-1}\int_k^E \beta'^2 F(E',k)dE'$. Changing the order of integration, $J(k) \propto \int_k^\infty dE' \ \ldots \int_{E'}^\infty E^{-\delta-1}dE$, and integrating over dE we obtain the results in equation (20).

On Figure (3) we have plotted $k^{\delta-1}J(k) \times \left(\frac{2\pi\delta\ell n\Lambda}{K\alpha}\right)$ versus photon energy k for various values of $\delta$. The slow (logarithmic) variation of these curves with k shows that for an isotropic electron distribution in a homogeneous medium, the observed IXB spectrum will have a spectral index[4] $\varphi \equiv -\frac{d \log J}{d \log k} \approx \delta-1$ for all energies. (For x-ray energies between 10 to 100 kev, $\varphi = \delta-0.9$.) As mentioned earlier, there appears to be a cutoff in the observed spectra of IXB's for photon energies greater than $\sim$ 100 kev or for $k \geq 0.2$. In the isotropic model one must therefore assume that the electron flux (equation 19) steepens for energies greater than 100 kev.

However, if we are observing bremsstrahlung radiation from a beam of electrons, the spectrum will depend on the angle $\theta$ between the beam and the line of sight. To illustrate this point, we have plotted the ratio

$$R_1(k,\theta) = \frac{J(k,\theta)}{J(k)} \times \left(\frac{4\pi}{d\Omega}\right) \qquad (21)$$

versus k for various values of $\cos\theta$ on Figure 4. As is evident from the curves on this figure, there appears to be a change in the spectral index around x-ray energies of 100 kev, except for $\theta \approx 0$. We approximate these spectra by two power laws; one for photon energies between 20 and 70 kev ($.04 \leq k \leq 0.14$) and one for photon energies > 100 kev and show in Table 1 the value of the quantity $\varphi-\delta+1$, a quantity nearly independent of $\delta$ (cf. Figure 4). The variation of $\varphi-\delta+1$ (or $\varphi$) with $\theta$ indicates that on the average there should be little difference between the spectrum of limb flares and flares observed on the center of the disk; but in every case the spectrum steepens ($\varphi$ increases by about one unit) for energies greater than 100 kev. The expected difference between the spectral indices for photons between 10 to 100 kev and for photons with energies > 100 kev

[4] The photon spectrum J(k) represents the energy per second per energy interval, not the number of photons per second per energy interval. (The spectral index for the latter is equal to $\varphi + 1$.)

would be larger than calculated here due to dependence on particle energy of the angle $\theta$. For example, for a beam of particles spiraling along a radial magnetic field, the angle $\theta$ is equal to the pitch angle $\psi$ of the particles for a flare at the center of disk. If the pitch angle $\psi$ of the particle is decreasing with increasing energy (cf. e.g. Speiser, 1965), the cutoff beyond 100 kev will be accentuated. (See also Brown, 1972, for the discussion of a model based on this assumption.) Furthermore, the lower energy x-rays are emitted by particles which have lost some of their energy through collisions. These collisions not only cause the loss of particle energy but also tend to isotropize the distribution of the electrons with a time constant comparable to the energy loss time. Thus lower energy electrons will be less directional than the higher electrons so that higher energy x-rays will tend to be beamed by larger factors (relative to low energy x-rays) than those calculated here.

Figure (5) shows variation of the quantity $R_1(k,\theta)$ with $\theta$ for various values of photon energy. The curves here imply that there should be a gradual increase of the IXB intensity relative to the H$\alpha$ or soft x-ray intensities as we go from flares from the center of the solar disk to flares near the limb. There has been some discussion of dependence on heliographic longitude of intensities of solar x-rays of different energies (cf. Phillips 1973 and references cited therein; Note that the approximate expression used by these authors for the dependence of the x-ray intensity on angle is significantly different from the exact calculations of the present paper). However, in the model under consideration here only the emission during the impulsive phase ($\sim$ 10 sec) will have directionality. The x-ray emission during the slower phase is due to thermal bremsstrahlung and therefore emitted isotropically. As more data on IXB's becomes available, the absence of existence of the correlation predicted by curves on Figure (5) can be used as a test for this model.

## IV. TOTAL ENERGY OF A FLARE

In this section we describe the derivation of the total energy of the accelerated electrons from the observed spectrum of the IXB's. In order to do this we calculate the yield of x-rays from the power law electron flux of equation (19). Since most of the energy resides in the lower energy part of the spectrum, the value of the low energy cutoff is important. Let us assume that the electron flux is given by equation (19) for energies $E \geq E_1$ and $dJ_e(E) = 0$ for $E < E_1 \ll 1$, so that the total flux $J_e$ and the total energy $\mathcal{E}_e$ (in units of $mc^2$) of the accelerated electrons are

$$J_e = \frac{K}{\delta} E_1^{-\delta} \text{ particles/sec} ,$$

$$\mathcal{E}_e = \frac{K}{\delta-1} E_1^{-\delta+1} \text{ sec}^{-1} . \qquad (23)$$

Since for most IXB's the value of $\delta$ ($\approx \varphi + 1$) varies from 2 to 5 (cf. Kane, 1971), the presence or absence of a high energy cutoff in the electron spectrum will not affect the results in this section.

For calculation of the radiation yield, we begin with equations (14) which gives the ratio of radiation to collision loss of an electron of energy $E$. Because the spectrum of IXB's are steep, most of the x-ray energy is emitted at low energies $k \approx E_1 \ll 1$ where the effect of the beaming is not overwhelming. We therefore first neglect the angular dependence and use the non-relativistic expression for the bremsstrahlung cross section. Calculations similar to this have been done by Lin and Hudson (1970) and by Syrovatskii and Shmeleva (1973) whose results differ from each other by an order of magnitude. We shall explain the origin of some of the errors giving rise to this discrepancy.

With the non-relativistic expression for the bremsstrahlung process, the integrated (over all directions) radiation yield is

$$Y(E,k) = \left(\frac{\alpha}{2\pi \ell n \Lambda}\right) \times \frac{16}{3} \log \frac{1 + \sqrt{1-k/E}}{1 - \sqrt{1-k/E}}, \qquad (24)$$

and the total yield is

$$Y(E') = \int_0^{E'} Y(E',k)dk = \frac{32}{3}\left(\frac{\alpha}{2\pi \ell n \Lambda}\right) E' . \qquad (25)$$

For a thin target, $Y(E')$ in equation (25) gives the ratio of the total bremsstrahlung radiation to collision losses of an electron of energy $E'$. In the present model, the target is thick and an electron of initial energy $E$ loses all of its energy, a fraction

$$Y(E) = \frac{1}{E} \int_0^{E} Y(E')dE' = \frac{16}{3}\left(\frac{\alpha}{2\pi \ell n \Lambda}\right) E \qquad (26)$$

of which is radiated. The radiation yield in a thick target is one half of that in a thin target (which was the case considered by Lin and Hudson,[5] 1970) because the radiation yield decreases as the electron is slowed down. The total radiation yield for a flux of electrons with the spectrum given above is therefore

$$Y(\delta) = \int_{E_1}^{\infty} EY(E)\, dJ_e(E)/\mathcal{E}_e = \frac{16}{3}\left(\frac{\alpha}{2\pi \ell n \Lambda}\right) E_1 \left(\frac{\delta-1}{\delta-2}\right) . \qquad (27)$$

(For the thin target case the ratio of bremsstrahlung to collision loss rates is equal to $\frac{32}{3}\left(\frac{\alpha}{2\pi \ell n \Lambda}\right) E_1 \frac{\delta}{\delta-1}$ .)

The quantity $Y(\delta)$ gives the total radiation yield; only a fraction of this radiation is in the observable x-ray energy ranges. As shown by

---

[5] From equation (13), in the non-relativistic limit, we obtain for the total bremsstrahlung loss rate $-\int \dot{E}_{brem} mc^2 dk = \frac{16}{3} \alpha r_o^2 n \times c\beta \times mc^2 = 2.9 \times 10^{-15} n\ (E/kev)^{1/2}$ kev/sec, which is a factor of 2 smaller than the rate given by these authors. This, along with the fact that they use the yield in a thin target, means that their results are larger than the yield in a thick target by a factor of 4.

the broken lines in Figure 3 (which show the x-ray spectrum expected from a power law electron spectrum with a low energy cutoff at 22 kev or $E_1 = .043$), most of the bremsstrahlung radiation is emitted at x-ray energies less than the cutoff energy $E_1$. (Note that what is plotted on this figure is $J(k)k^{\delta-1}$ so that $J(k)$ is still rising initially for $k < E_1$.) These spectra are obtained from equation (20) for $k > E_1$ and for $k < E_1$ we have (for the non-relativistic case)

$$J(k) = \frac{16}{3}\frac{\alpha}{2\pi \ell n \Lambda} J_e \left\{ \int_k^{E_1} \ell n \frac{1+\sqrt{1-k/E'}}{1-\sqrt{1-k/E'}}\, dE' + \int_{E_1}^{\infty} \left(\frac{E'}{E_1}\right)^{-\delta} \ell n \frac{1+\sqrt{1-k/E'}}{1-\sqrt{1-k/E'}}\, dE' \right\} . \tag{28}$$

The total yield, as given in equation (27), is obtained if we integrate $J(k)$ over all $k$; i.e. $Y(\delta) = \frac{1}{\mathcal{E}_e}\int_o^{\infty} J(k)dk$. The yield of photons of energy $k \geq E_1$ is, on the other hand, given by

$$Y(k \geq E_1, \delta) = \frac{1}{\mathcal{E}_e}\int_{E_1}^{\infty} J(k)dk = \frac{16}{3}\frac{\alpha}{2\pi \ell n \Lambda}\frac{J_e}{\mathcal{E}_e} E_1^2 \int_{E_1}^{\infty}\left(\frac{E}{E_1}\right)^{-\delta+1}\frac{dE}{E_1}\int_{E_1}^{E} \ell n \frac{1+\sqrt{1-k/E}}{1-\sqrt{1-k/E}}\frac{dk}{E} . \tag{29}$$

The integral over $dk$ yields $2\sqrt{1-E/E_1} - \frac{E_1}{E}\ell n \frac{1+\sqrt{1-E_1/E}}{1-\sqrt{1-E_1/E}}$ which, within a few percent, can be approximated as $2(1-E_1/E)^2$. With this approximation we obtain

$$Y(k \geq E_1, \delta) = \frac{16}{3}\frac{\alpha}{2\pi \ell n \Lambda} E_1 \left(\frac{2}{\delta}\right)^2 \frac{1}{\delta-2} \tag{30}$$

which is smaller than the total yield (equation 27) by the factor[6]

---

[6] Note this quantity is related to the quantity G of Lin and Hudson (1970). If we neglect the difference between number of photons with $22 < k < 38$ kev and those with $k > 22$ kev (which is less than 20%) then $G \propto \frac{1}{R_2(\delta)}\frac{\varphi}{\varphi-1}$. We find that G varies rapidly with $\delta$ ($G \propto \delta^3$) and is larger than calculated by these authors by a factor ranging from 4 to 6. Note also that their $\delta$ and its relation to photon spectral index differs from ours.

$$R_2(\delta) = \left(\frac{2}{\delta}\right)^2 \frac{1}{\delta-1} \quad . \tag{31}$$

On Table II we give numerical values for $Y(\delta)$, $Y(k \geq E_1, \delta)$ and $R_2(\delta)$ for an ionized hydrogen medium ($\ell n\Lambda = 44$) and for $E_1 = 22$ kev. (For neutral hydrogen, $\ell n\Lambda = 16$, the numbers on Table II must be multiplied by 2.7.) On this table are also tabulated $Y(k \geq E_1, \delta)$ as obtained from the exact evaluation of equation (20). From the graphs of Figure (3), the rate of total energy (in units of $mc^2$) emission of x-rays of energy greater than $k_1$ is equal to

$$\int_{k_1}^{\infty} J(k)dk = \frac{\alpha}{2\pi\ell n\Lambda} \times \frac{K}{\delta} \times \frac{X(\delta,k_1)}{\delta-2} k_1^{-\delta+2} \ \text{sec}^{-1} \tag{32}$$

where $X$ is the value of the ordinate for the particular values of $k_1$ and $\delta$. The numbers in the last column give the ratio of the above quantity to $\mathcal{E}_e$:

$$Y(k \geq E_1, \delta) = \frac{\alpha}{2\pi\ell n\Lambda} E_1 \frac{\delta-1}{\delta-2} \times \frac{X(\delta,E_1)}{\delta} \quad . \tag{33}$$

As can be seen from comparison of columns (6) and (7), the analytic expression given in equations (27) to (31) are in excellent agreement with the results of the numerical integration.

All the expressions derived here relate the total radiated energies to electron energies. The ratios of number of photons radiated to number of non-thermal electrons can be obtained from expressions (27) to (33) and Table II by changing $\delta$ to $\delta+1$. Our results as shown on Table II agree with the calculation (for a thick target) by Syrovatskii and Shmeleva (1973) but give radiation yields 20 to 25 times smaller than those calculated by Lin and Hudson (1970) which is applicable for a thin target case and appears to contain

numerical errors as described in the preceding footnotes. Furthermore, the yields on Table II are calculated for $E_1 \simeq 22$ kev. If the electron spectrum is cut off at energies lower than this, the yield is reduced by a factor of $(E_1/22 \text{ kev})$.

We have considered so far the integrated (over all angles) yield. If the electrons are beamed toward the photosphere then, for a given electron spectrum, the x-ray radiation emitted toward the earth will be smaller than the average for $\theta > \pi/2$. The yield Y therefore is reduced by the ratio R in equation (21). From Figures (4) we find that for $\theta \approx \pi$ (and $E_1 =$ 22 kev) the yield $Y(k \geq 22 \text{ kev}, \delta)$ is reduced by factors of 5, and the total yield $Y(\delta)$ by a factor of 3. Both these factors approach unity as $\theta$ approaches $\frac{\pi}{2}$.

The results presented here can be used for determination of the total energy of non-thermal electrons. For a given observed spectral index and intensity I of an IXB, the total energy of the non-thermal electrons can be obtained from the following relation.

$$[\mathcal{E}_e(E \geq E_1)/\text{kev}] = 2.8 \times 10^{27} \text{cm}^2 \left(\frac{I(k \geq k_1)}{\text{kev cm}^2}\right)\left(\frac{k_1}{E_1}\right)^{\varphi} \Big/ [Y(k \geq k_1, \delta) \times R_1(k_1, \theta)] \,, \tag{34}$$

which is valid for $k_1 \geq E_1$.

For a typical flare ($\varphi \sim 3.5$) the quantity $2.8 \times 10^{27} I(k \geq 22 \text{ kev})$ is in the range from $(1\text{-}4) \times 10^{32}$ kev (Kane and Anderson, 1970; Lin and Hudson, 1970), so that when the effect of the beaming is neglected $\mathcal{E}_e(E \geq 22 \text{ kev}) \approx (3\text{-}12) \times 10^{24}$ ergs. If $\theta > 3\frac{\pi}{2}$ (which will be the case for flares near the center of the disk), including the effect of the beaming, we find that $\mathcal{E}_e(E \geq 22 \text{ kev}) \approx (1.5\text{-}6) \times 10^{30}$ ergs. Energies as large as $10^{32}$ ergs can be obtained if the spectrum of the electrons continues as a power law down to energies of 10 to 6 kev.

## V. DISCUSSION

We summarize here briefly our results. We have argued that if the high energy electrons responsible for the observed impulsive x-ray and microwave bursts are accelerated somewhere in the corona (as in models proposed by de Jager and Kundu 1963; Sturrock 1968) then only those electrons beamed toward the photosphere will be important in producing bremsstrahlung x-ray radiation. Consequently, we find a more realistic model of x-ray production is that where the radiation arises from a beam of high energy electrons directed into the stratified chromospheric plasma. Recent polarization measurements (Tindo et al., 1970) lend support to this model.

We have calculated the spectrum of x-rays resulting in such a model. We find that the effect of the "relativistic" beaming (which is already considerable for electrons with ten to hundreds of kev energy) is to (i) yield an observed x-ray spectrum (in the range 10 to 100 kev) which is steeper than when the beaming is neglected, and (ii) produce a relatively rapid cutoff in the spectrum for energies greater than 100 kev. The latter effect may explain the observed high energy cutoff in the spectrum of IXB's without requiring a cutoff in the spectrum of the high energy electron. We find the presence of such a cutoff unsatisfactory since particles of energies greater than the cutoff energy are needed for production of the microwave bursts.

We have also calculated the yield of radiation in this model. We present the results here in the form of general formulae which could be used for calculation of the total energy of the non-thermal electrons for an observed impulsive x-ray burst. These results show that there is sufficient energy in high energy electrons responsible for typical observed impulsive x-ray bursts to account for all of the energy radiated by large flares.

## ACKNOWLEDGMENTS

I would like to thank Drs. P.A. Sturrock and H. Hudson for many valuable discussions and Mr. Patrick Chye for his help with the numerical calculations. This work was supported by the National Aeronautics and Space Administration under Grant NGL 05-020-272.

TABLE I

Relation Between X-Ray and Non-Thermal Electron Spectral Indecies

$\varphi = \delta + 1$

| photon energy range \ $\cos\theta$ | -1 | -0.5 | 0.0 | +0.5 |
|---|---|---|---|---|
| $20 < k < 70$ kev | 0.50 | 0.55 | 0.40 | -0.1 |
| $k > 100$ kev | 1.2 | 1.3 | 1.2 | 1.0 |

TABLE II

Bremsstrahlung Radiation Yield in a Thick Target

| $\varphi = \phi - 1$ | $\delta$ | $Y(\delta)$ eq. (27) | $R_2(\delta)$ eq. (31) | $Y(k \geq 22$ kev, $\delta)$ | |
|---|---|---|---|---|---|
| | | | | eq. (30) | eq. (33) |
| 1.5 | 2.5 | $1.82 \times 10^{-5}$ | 0.427 | $7.8 \times 10^{-6}$ | $7.3 \times 10^{-6}$ |
| 2.0 | 3.0 | 1.21 | 0.222 | 2.7 | 2.6 |
| 2.5 | 3.5 | 1.01 | 0.131 | 1.3 | 1.3 |
| 3.0 | 4.0 | 0.91 | 0.083 | 0.76 | 0.71 |
| 3.5 | 4.5 | 0.85 | 0.056 | 0.48 | 0.51 |
| 4.0 | 5.0 | $0.81 \times 10^{-5}$ | 0.040 | $0.32 \times 10^{-6}$ | $0.32 \times 10^{-6}$ |

Note: $\delta$ is the exponent of electron spectrum as defined in equation (19); $\varphi \approx \delta - 1$ is the exponent of x-ray spectrum $J(k) \propto k^{-\varphi}$ kev kev$^{-1}$sec$^{-1}$; $\phi = \varphi + 1$ is the exponent for the number (not energy) of photons per unit energy interval; $n_x(k) \propto k^{-\phi}$ photons kev$^{-1}$sec$^{-1}$.

## REFERENCES


Benz, A. O., and Gold, T. 1971, Sol. Phys., 21, 157.

Berger, M. J., and Seltzer, S. M. 1964, "Tables of Energy Losses and Ranges of Electrons and Positrons", NASA SP-3012.

Brown, J. C. 1971, Sol. Phys., 18, 489.

_____. 1972, ibid, 25, 158.

Elwert, G. 1939, Ann. Phys., 34, 178.

Elwert, G., and Haug, E. 1971, Sol. Phys., 20, 413.

Frost, K. 1969, Ap. J. (Letters), 158, L159.

Ginzburg, V. L., and Syrovatskii, S. I. 1964, "Origin of Cosmic Rays" (Pergamon Press, N.Y.).

Hayakowa, S., and Kiato, K. 1956, Prog. Theoretical Phys., 16, 139.

Holt, S. S., and Ramaty, R. 1969, Sol. Phys., 8, 119.

Hudson, H. S. 1972, Sol. Phys., 24, 414.

deJager, C., and Kundu, M. R. 1963, Space Res., 3, 836.

Kane, S. R. 1971, Ap. J., 170, 587.

_____. 1972, Sol. Phys., 27, 174.

Kane, S. R., and Anderson, K. A. 1970, Ap. J., 162, 1003.

Koch, H. W., and Motz, J. W. 1959, Rev. Mod. Phys., 31, 920.

Lin, R. P., and Hudson, H. S. 1971, Sol. Phys., 17, 412.

Phillips, K. J. H. 1973, The Observatory, 93, 17.

Speiser, T. W. 1965, J. Geophys. Res., 20, 4219.

Spitzer Jr., L. 1956, "Physics of Fully Ionized Gases" (Interscience Publishers, New York).

Sturrock, P. A. 1968, "Structure and Development of Solar Active Regions" (Holland: Reidel), p. 95.

Syrovatskii, S. I., and Shmeleva, O. P. 1973, Sov. Astron. AJ, 16, 273.

Takakura, T. 1972, Sol. Phys., 26, 151.

Takakura, T., and Kai, K. 1966, Pub. Soc. Japan, 18, 57.

_____. 1969, Sol. Phys., 6, 133.

Tindo, I. P., Ivanov, V. D., Mandelstam, S. L., and Shurighin, A. I. 1970, Sol. Phys., 14, 204.

## FIGURE CAPTIONS

Figure 1. Decay time of electrons versus their energy in stratified atmosphere of ionized hydrogen with density scale height H. $n_o$ is the ambient density at the point of injection of electrons.

Figure 2a. The ratio of bremsstrahlung radiation per sterradian in a direction $\theta$ with respect to their direction of motion, to the average bremsstrahlung radiation per sterradian. The curves are labeled by the initial energy E of the electron (in kev); the photon energy $k = 0.681E$.

Figure 2b. Same as Figure 2a but with $k = 0.316E$.

Figure 2c. Same as Figure 2a but with $k = 0.1E$.

Figure 3. The spectrum $J(k)$ of average (over all directions) bremsstrahlung radiation from an electron beam with a power law spectrum. $\delta = d \log J_e / d \log E$, where $J_e(E)$ is the flux of electrons with energies greater than E. The dashed lines are for an electron power spectrum with a sharp cutoff at $E < 22$ kev.

Figure 4. The ratio of bremsstrahlung radiation per sterradian in a direction $\theta$ to the average radiation per sterradian. $\theta$ is the angle between line of sight and the direction of the electron beam described on Figure 3; solid lines for $\delta = 3$, dashed lines for $\delta = 5$. The curves are labeled by the value of $\cos\theta$. For $\cos\theta = 1$ multiply the ordinate by 10 to obtain the actual value for $R_1(k, \theta=0)$.

Figure 5. Same as Figure 4 except here the quantity $R_1$ has been plotted versus $\cos\theta$ for various photon energies (in kev); $\delta = 4$.

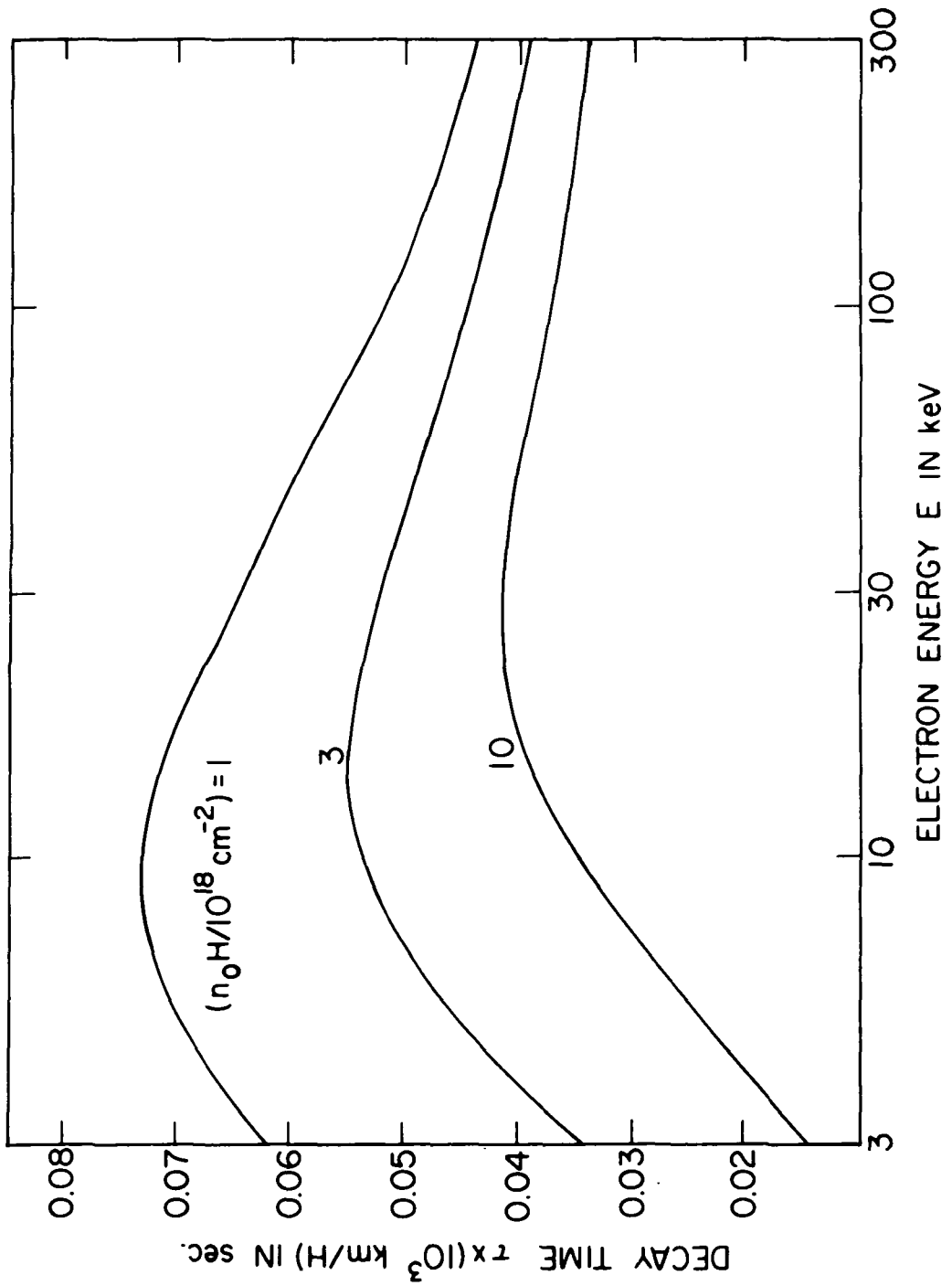
DECAY TIME τ x(10³ km/H) IN sec.
0.08
0.07
0.06
0.05
0.04
0.03
0.02
3
10
30
100
300
ELECTRON ENERGY E IN keV
$(n_oH/10^{18}cm^{-2})=1$
3
10

Figure 1

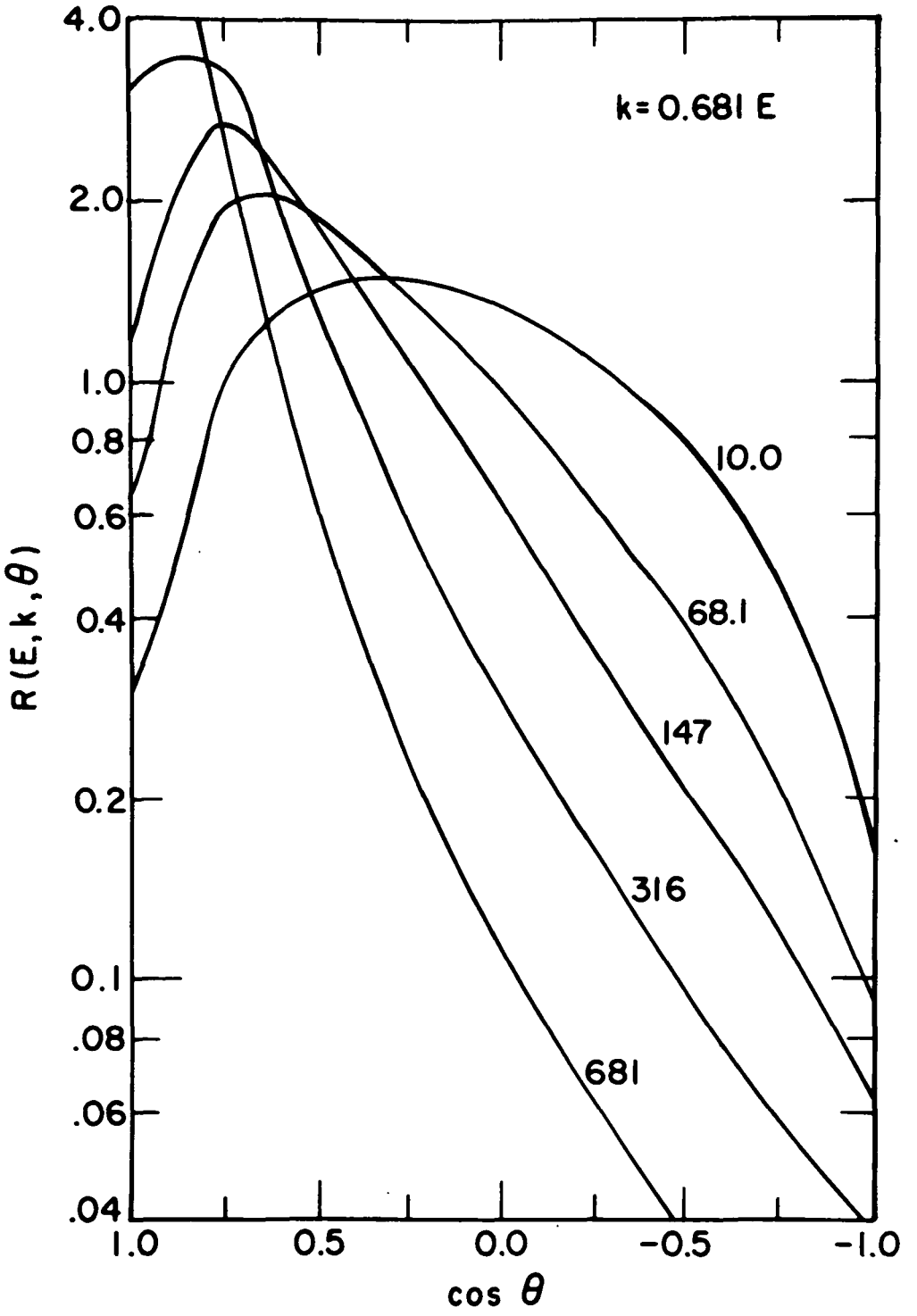
4.0
2.0
1.0
0.8
0.6
0.4
0.2
0.1
.08
.06
.04
k= 0.681 E
10.0
68.1
147
316
681
R(E, k, θ)
1.0
0.5
0.0
-0.5
-1.0
cos θ

Figure 2a

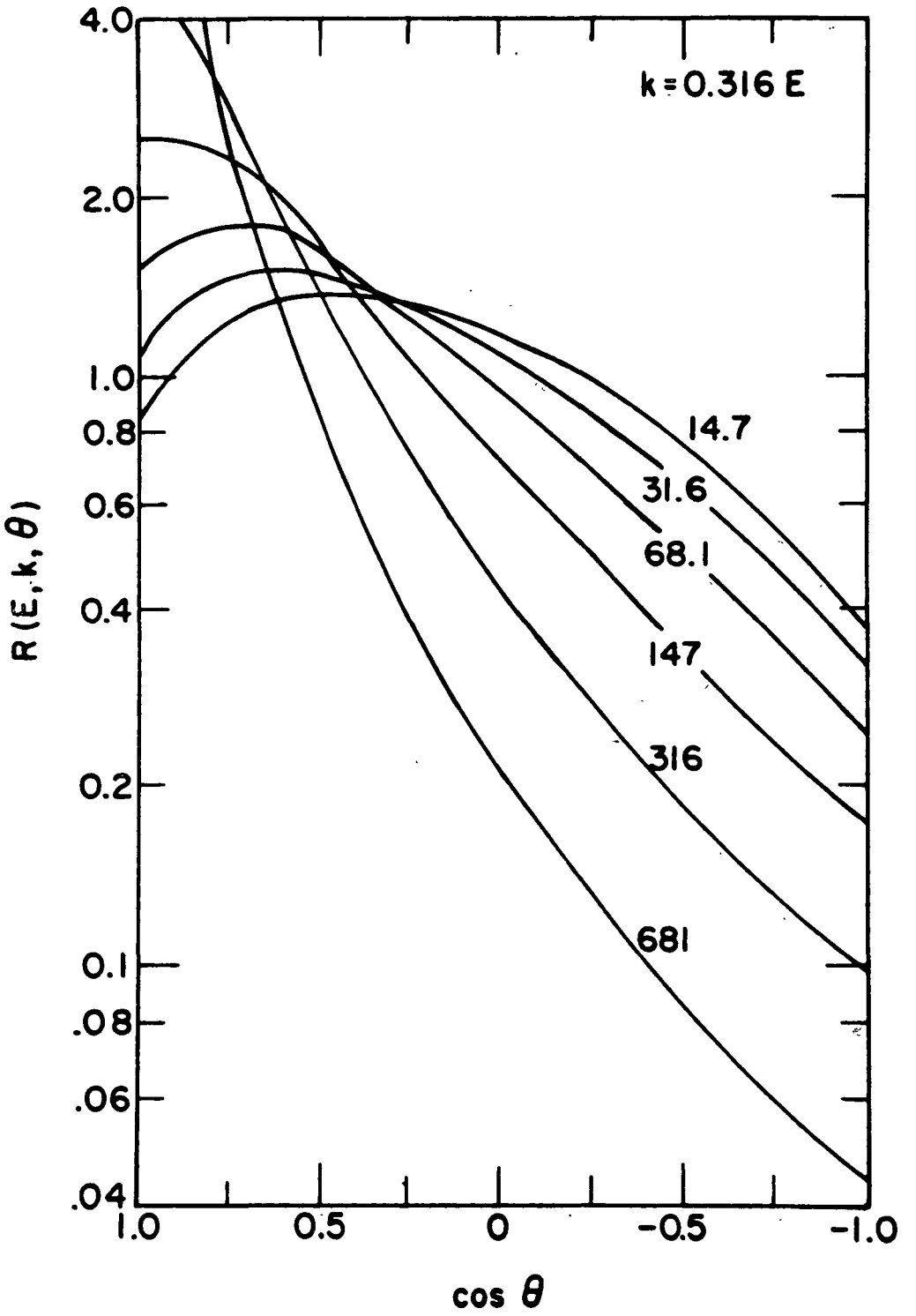
k = 0.316 E
14.7
31.6
68.1
147
316
681
4.0
2.0
1.0
0.8
0.6
0.4
0.2
0.1
.08
.06
.04
1.0
0.5
0
-0.5
-1.0
R(E, k, θ)
cos θ

Figure 2b

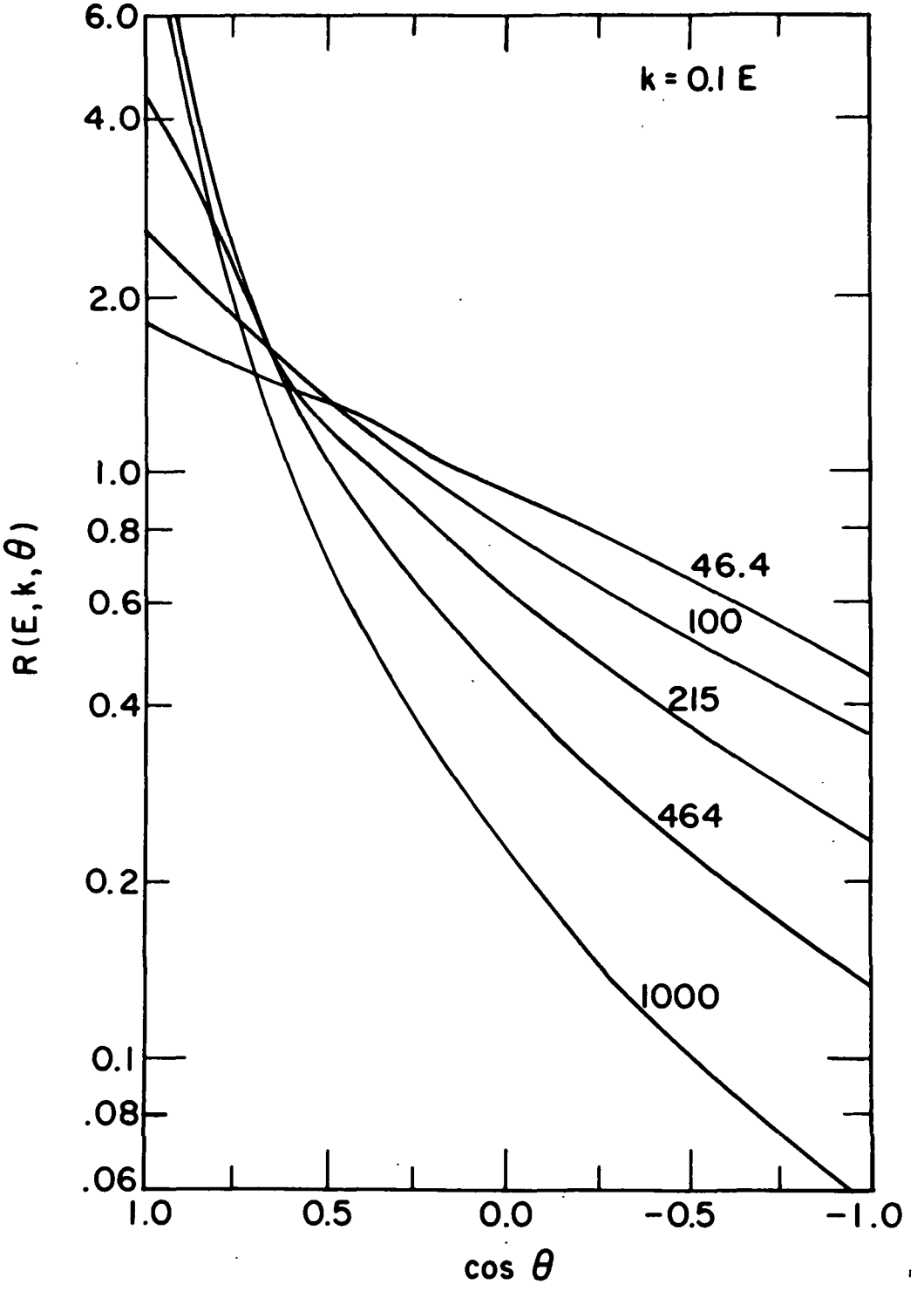
k = 0.1 E
6.0
4.0
2.0
1.0
0.8
0.6
0.4
0.2
0.1
.08
.06
R(E, k, θ)
46.4
100
215
464
1000
1.0
0.5
0.0
-0.5
-1.0
cos θ

Figure 2c

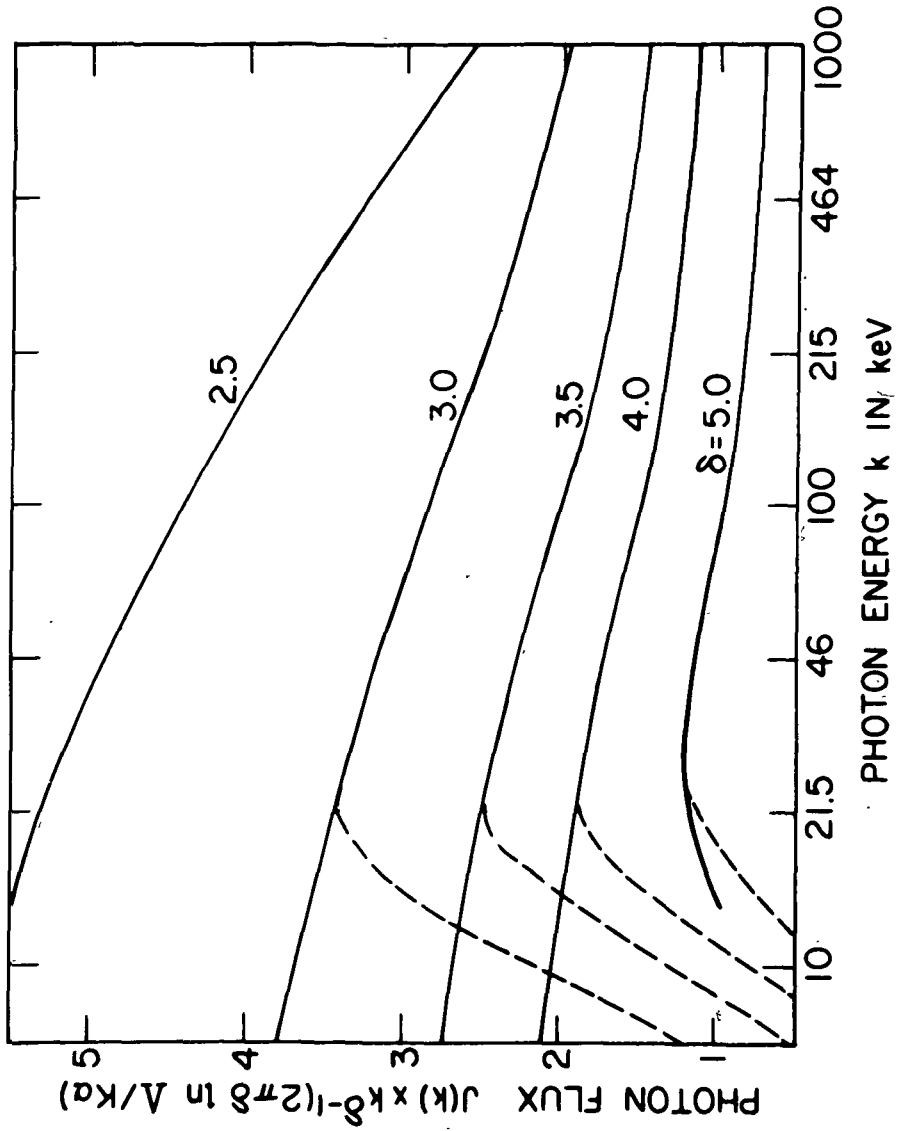
PHOTON FLUX J(k) x k^δ-1(2πδ ln Λ/Ka)
PHOTON ENERGY k IN keV
1
2
3
4
5
10
21.5
46
100
215
464
1000
2.5
3.0
3.5
4.0
δ=5.0

Figure 3

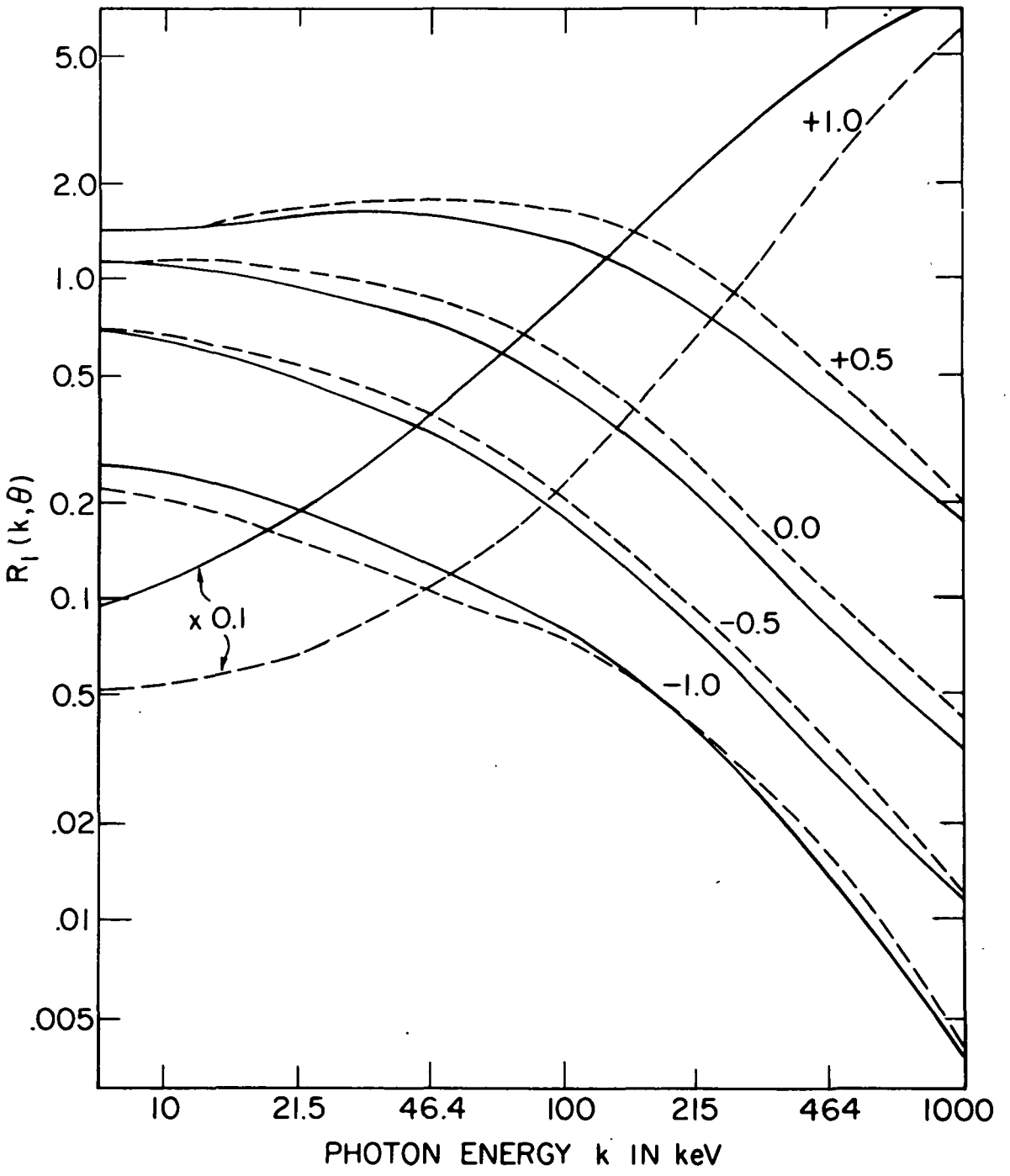
5.0
2.0
1.0
0.5
0.2
0.1
0.5
.02
.01
.005
$R_1(k,\theta)$
+1.0
+0.5
0.0
-0.5
-1.0
x 0.1
10
21.5
46.4
100
215
464
1000
PHOTON ENERGY k IN keV

Figure 4

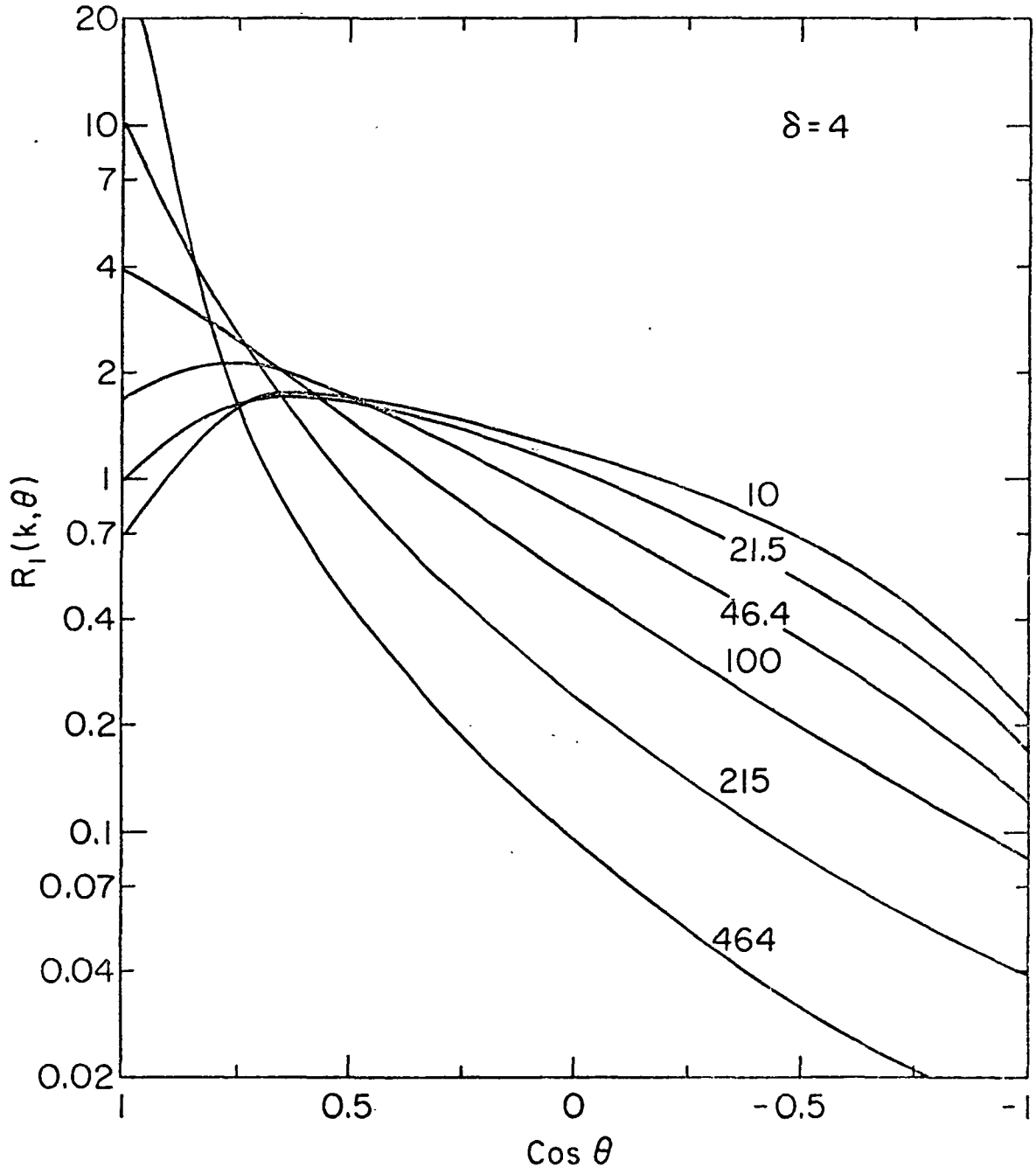
20
10
7
4
2
1
0.7
0.4
0.2
0.1
0.07
0.04
0.02
δ = 4
10
21.5
46.4
100
215
464
R1(k,θ)
1
0.5
0
-0.5
-1
Cos θ

Figure 5